East Eur. J. Phys. Vol.2 No.2 (2015) 51-58

PACS: 87.14.Cc, 87.16.Dg

MODELING OF AMYLOID FIBRIL BINDING TO THE LIPID BILAYER

V. Trusova
Department of Nuclear and Medical Physics, V.N. Karazin Kharkov National University
4 Svobody Sq., Kharkov, 61022, Ukraine
e-mail: valtrusova@yahoo.com
Received June 9, 2015

Using the different computational approaches, we constructed the core region of amyloid fibrils from lysozyme, Aβ-protein and apolioprotein A-I, and studied the adsorption of fibrillar aggregates onto lipid bilayer surface. The structures of amyloids differing in their twisting angle were generated with CreateFibril software. The stability of the obtained assemblies was assessed by means of AQUASOL tool, and the twisting angle providing the most stable conformation was identified. The energetically favorable orientation of the fibrils within the lipid membranes was predicted based on PPM server. It was found that increasing amyloid periodicity bring about the rise in free energy of peptide transfer from aqueous to membrane phase.
KEYWORDS: amyloid fibrils; twisting angle; polymorphism; membrane orientation; computational modeling

МОДЕЛЮВАННЯ ЗВ'ЯЗУВАННЯ АМІЛОЇДНИХ ФІБРИЛ З ЛІПІДНИМ БІШАРОМ

В. Трусова
Кафедра ядерної та медичної фізики, Харківський національний університет ім. В.Н. Каразіна
пл. Свободи 4, Харків, 61022, Україна

За допомогою різних методів комп'ютерного моделювання було сконструйовано амілоїдні фібрили лізоциму, Аβ-білка та аполіпопротеїну А-І, а також було досліджено сорбцію фібрилярних агрегатів на поверхню ліпідного бішару. Структури амілоїдних фібрил, які відрізнялися за своїм кутом закручення, було згенеровано за допомогою програми CreateFibril. Стабільність отриманих агрегатів була оцінена на основі серверу AQUASOL. Енергетично оптимальна орієнтація фібрилярних агрегатів на мембрані була ідентифікована за допомогою серверу PPM. Знайдено, що зростання періодичності амілоїдів приводить до збільшення вільної енергії переносу пептидів з водної фази в ліпідну.
КЛЮЧОВІ СЛОВА: амілоїдні фібрили; кут закручування; поліморфізм; орієнтація у мембрані; комп'ютерне моделювання

МОДЕЛИРОВАНИЕ СВЯЗЫВАНИЯ АМИЛОИДНЫХ ФИБРИЛЛ С ЛИПИДНЫМ БИСЛОЕМ

В. Трусова
Кафедра ядерной и медицинской физики, Харьковский национальный университет им. В.Н. Каразина
пл. Свободы 4, Харьков, 61022, Украина

С помощью различных методов компьютерного моделирования были сконструированы амилоидные фибриллы лизоцима, Аβ-белка и аполипопротеина А-I, а также было изучена сорбция фибриллярных агрегатов на поверхность липидного бислоя. Структуры амилоидных фибрилл, которые отличались углом закручивания, были сгенерированы с помощью программы CreateFibril. Стабильность полученных агрегатов была оценена на основании сервера AQUASOL. Энергетически оптимальная ориентация фибриллярных агрегатов на мембране была идентифицирована с помощью сервера PPM. Показано, что увеличение периодичности амилоидов приводит к возрастанию свободной энергии переноса пептидов из водной в липидную фазу.
КЛЮЧЕВЫЕ СЛОВА: амилоидные фибриллы; угол закручивания; полиморфизм; ориентация в мембране; компьютерное моделирование

The self-assembly of specific proteins and peptides into highly ordered supramolecular aggregates (amyloid fibrils) is currently attracting a growing interest in a variety of research areas from biomedicine to nanotechnology [1,2]. The unique physical and structural properties of amyloid fibrils make them the promising candidates for the design of novel functional materials and devices [3]. However, the main focus in amyloid research is essentially shifted towards elucidating the role of fibrillar assemblies in pathogenesis of so-called conformational diseases, such as neurological disorders (Parkinson's, Alzheimer's and Huntington's diseases), type II diabetes, systemic amyloidosis, spongiform encephalopathies, etc. [4]. The impairment of cell functions by fibrillized proteins and intermediates is causatively linked to the complex conformational behavior of these aggregates, which are distinguished by the presence of a core cross-β-sheet structure with β-strands orienting perpendicularly to the fibril long axis and β-sheets propagating in its direction [1]. Such molecular architecture is stabilized by the main-chain hydrogen bonding, ionic pairing, van der Waals, aromatic π-π interactions and hydrogen bonds between amino-acid side chains [5-7]. Another fundamental feature of fibrillar state is associated with the formation of topologically distinct structures, such as twisted ribbons, helical ribbons and nanotubes [8]. The twisting ability of amyloid is controlled by chirality [9,10], electrostatics [11,12], as well as entropic contributions arising from solvent rearrangement around side chains and backbone dynamics [11]. Importantly, the morphology of amyloid assemblies is supposed to be an essential determinant of their cytotoxicity [13].

Ample evidence suggests that toxic action of fibrillar aggregates is primarily targeted at cell membranes [14]. It was demonstrated that amyloid-induced cellular dysfunction may result from the alterations in membrane integrity and physicochemical characteristics, involving the changes in lipid bilayer permeability, lipid loss, receptor activation,

membrane fragmentation, etc. [15], with the extent of membrane perturbations being dependent on structural properties of the protein aggregates [16]. Subtle modifications in growth conditions along with different modes of intramolecular and side-chain interactions may produce a wide collection of amyloid polymorphs with distinct molecular architecture formed by the same amino acid sequence [12]. In view of this, establishing a correlation between the structural peculiarities of amyloid aggregates and their ability to interact with lipid bilayer and modify its structure seems to be of outmost importance for uncovering the molecular details of fibril cytotoxicity. Since experimental solving of this problem is still hardly feasible, increasing attention is given to computational analytical tools. The present contribution is devoted to exploring the interactions of different structural variants of amyloid fibrils with lipid membranes using the computer modeling approach. Our goal was threefold: i) using the computational framework of CreateFibril web resource to construct the polymorphic amyloid fibrils of hen egg white lysozyme, Aβ, and apolipoprotein A-I peptides, differing in their twisting angle; ii) to assess the stability of constructed fibrils in water with AQUASOL tool and to identify the most energetically favorable polymorphs; iii) to predict the mode of amyloid association with lipid bilayer using the PPM web server.

CONSTRUCTION AND STABILITY OF PEPTIDE AMYLOID FIBRILS

CreateFibril tool was used to construct the amyloid fibrils of the peptides from hen egg white lysozyme, Aβ and apoliprotein A-I [17]. More specifically, the analyzed peptide sequences involve:

- K-peptide of lysozyme, GILQINSRW, residues 54-62 of wild-type protein, (**Lz1**),
- derivative of K-peptide, IFQINS (**Lz2**),
- peptide (residues 24-50) from G26R-mutated apolipoprotein A-I, DSRRDYVSQFEGSALGKQLNLKLLDNW (**A-I**)
- peptide from Aβ protein, LVFFAEDVGSNKGAIIGLMVGGVVIA, residues 17-42 of Aβ (**Aβ**).

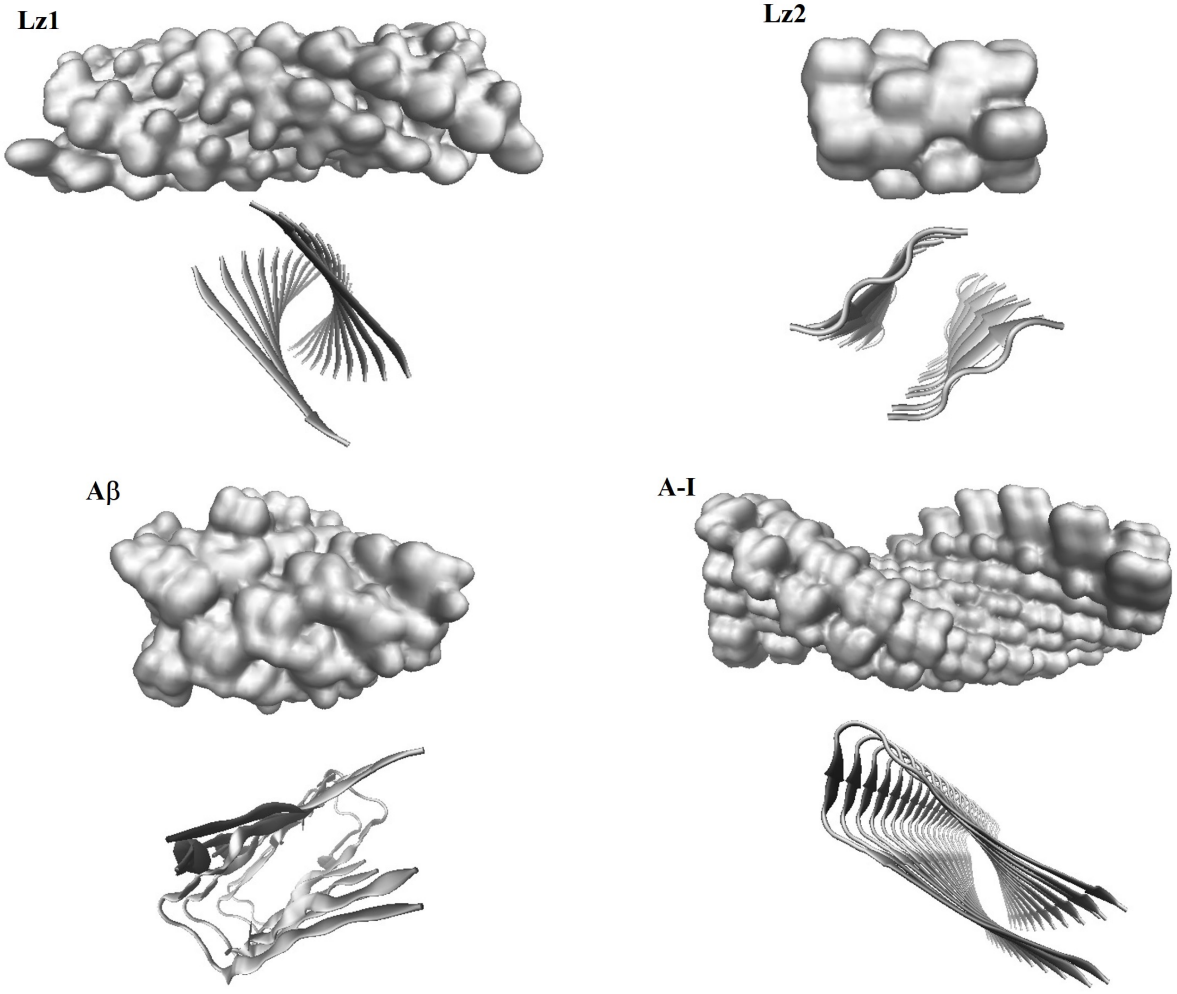

Fig. 1. Side and cross-sectional view of the fibrils constructed with the use of CreateFibril software.

The structure of **Lz1** dimer, used as input for CreateFibril, was generated from Lz1 monomer in β-strand conformation with PatchDock and FireDock tools [18,19]. **Lz2** dimer was obtained in similar way but monomeric structure was taken from Protein Data Bank (PDB code 4R0P). **A-I** dimer was created as described in [20], while **Aβ**

tetramer was taken from Protein Data Bank (PDB code 2BEG). The choice of the peptides **Lz1**, **A-I** and **Aβ** was dictated by the fact that they represent the core of the amyloid fibrils from corresponding proteins. Peptide **Lz2** was used to bring out the effect of amino acid sequence on the amyloid stability and fibril-lipid interactions.

The mathematical background of CreateFibril software involves translational and rotational affine transformations which allow creating several identical copies of the fibril fragment and stacking them side-by-side, elongating thereby the fibrillar aggregate [18]. The procedure of the fibril constructing requires the following parameters: i) the number of protofilaments and their packing distance perpendicular to fibril axis, n and R, respectively; ii) the direction of fibril axis; iii) the fibril length (the number of monomers), r; iv) the distance between β-strands along the fibril axis, d; v) the rotation angle of amyloid monomers along the fibril axis (twisting angle), θ. While creating the amyloid structures studied here, the parameters R and d were taken as 5 Å, n was 2, 4, 1 and 2 for **Lz1**, **Lz2**, **Aβ** and **A-I**, respectively. Parameter r was set as 4 for **Aβ** and 10 for the rest of the peptides. Rotation angle was allowed to vary from 0 to 40° degrees (with a 5° step). The differences in the input parameters are explained by the distinct structural features and amyloid-forming propensities of the examined peptides. Such kind of modeling yields nine fibrillar structures for every peptide, whose representative pictures are given in Fig. 1. As seen from this figure, the constructed fibers are characterized by repeated intertwined structure, enriched in β-sheets, which represents the hallmark of amyloid aggregates.

The next step of the study was directed towards assessing the stability of created fibrillar structures. To achieve this goal, the free energies of the fibrils were computed in water as a sum of Lennard-Jones, Coulomb and solvation energies using the AQUASOL server [21]. Specifically, this program solves the dipolar Poisson-Boltzmann-Langevin (DPBL) equation for a given system. In DPBL formalism the solvent is represented as a collection of orientable dipoles with nonuniform concentration. This results in nonlinear dependence of permittivity on the atom position and local electric field at this position. DPBL approach is supposed to be the most adequate in calculating the energetic profiles of biomolecules. The solution of DPBL equation yields the electrostatic potential at each position. The procedure of AQUASOL simulations includes, first, the hydration of amyloid fibrils and their equilibration in water followed by calculations of the free energies. The recovered dependencies of the fibril energy on its twisting angle are presented in Fig. 2. Analysis of these profiles showed that the most stable fibrillar aggregates have the twisting angles of 15, 5, 20 and 20° for **Lz1**, **Lz2**, **Aβ** and **A-I**, respectively.

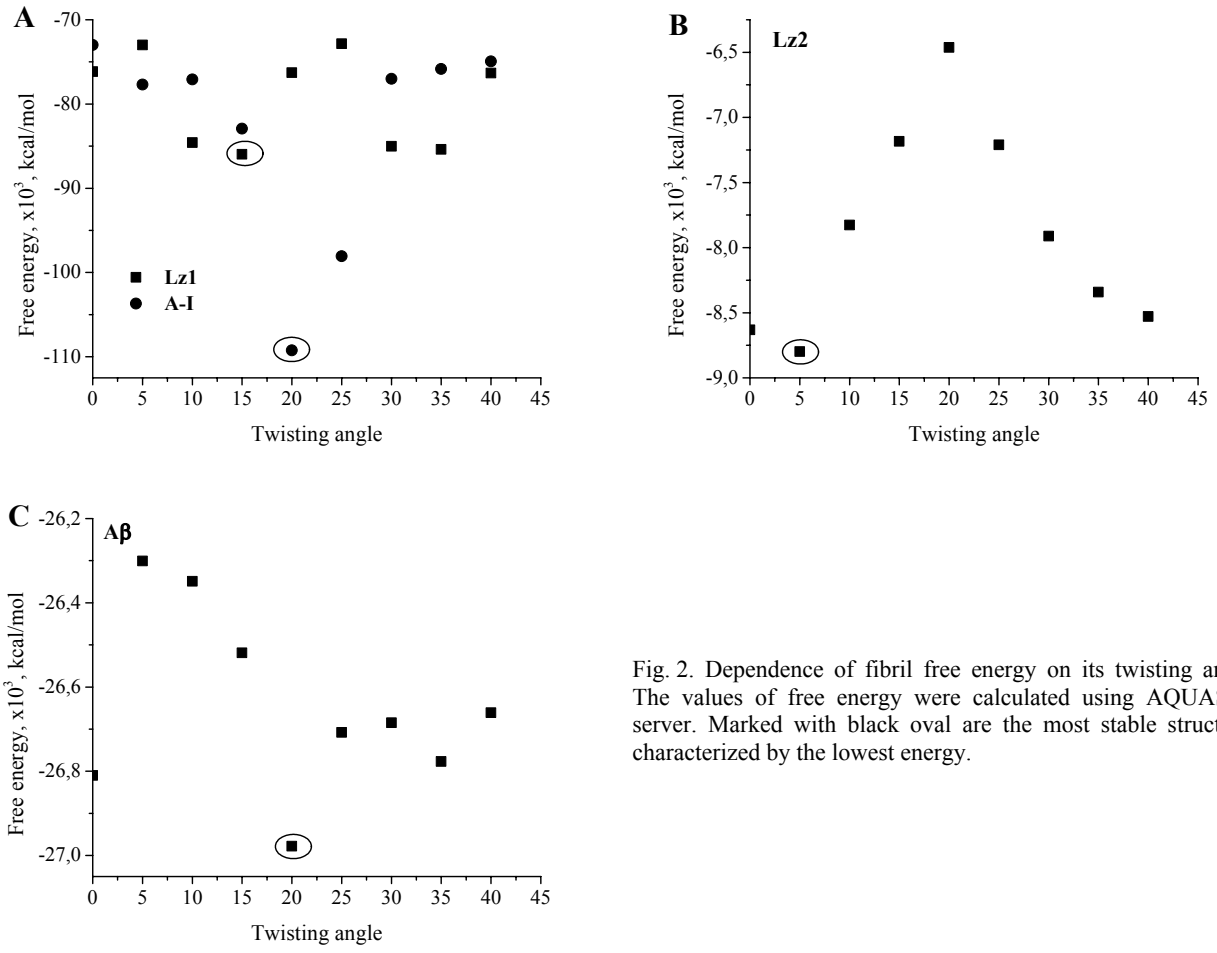

Fig. 2. Dependence of fibril free energy on its twisting angle. The values of free energy were calculated using AQUASOL server. Marked with black oval are the most stable structures characterized by the lowest energy.

In the present context it is worth of mentioning that molecular origin of the amyloid twist is still a matter of extensive debates. Originally, the main reason for the intertwining of the protofibrils is thought to be the intrinsic chirality of amino acid residues [22]. However, further progress in amyloid physics showed that twisting of fibrillar aggregates arises from the balance between fibril elasticity and electrostatic repulsion [23]:

$$U = \frac{1}{2} M\theta^2 + \frac{k_B T 2\pi\nu^2 Q e^{-\kappa D}}{\kappa \sin\theta}, \quad (1)$$

where U is the total energy of the twisting, M is the torsional modulus of the fibrils, ν, κ and Q denote the linear charge density of the fibril, the inverse Debye length and the Bjerrum length, respectively, θ is the twist angle. The first term in this equation represents the elastic torsional energy, which opposes the twist, while the second term stands for screened electrostatic potential of the twisted fibrils, which promotes the twist. In a flat configuration the distance between the charges of the same sign may not be sufficient to compensate the energetic costs connected with the electrostatic repulsion. In turn, rotation around the long axis increases the distance between the charges, minimizing thereby the electrostatic repulsion. However, increased separation between the consecutive polypeptide segments creates the penalty in elastic energy favoring the flattered configuration. The final twist of the amyloid fibril is determined by the delicate balance between the above processes.

The widely accepted model of amyloid structure assumes that the stacked pleated β-sheets are twisted in such a way that a repeating unit of 24 β-strands constitutes a full helical turn around the fibril axis [24]. Such a configuration generates the twist of 15° between the neighboring β-strands. The twisting angles 15-20° recovered here for the most stable configurations of **Lz1**, **Aβ** and **A-I** fibrils are in a good harmony with the above model. The only exception is **Lz2** fibrils, for which the most stable structure corresponds to the twisting angle 5°. This finding may be explained by the small length of the constructed fibrils which does not allow the high twist angle, since in this case the large elastic energy penalty is created. However, it is expected that propagation of the fibril would shift the twisting angle, that characterizes the most stable structure, to the higher values.

MODELING OF AMYLOID FIBRIL ASSOCIATION WITH LIPID MEMBRANES

In the following, it was of interest to simulate the adsorption of the constructed fibrillar aggregates onto the lipid bilayer. In view of the crucial role of fibril-induced membrane disruption in amyloid cytotoxicity, the analysis of protein aggregate orientation within the membrane may be of particular importance for elucidating the molecular-level details of their destructive effect. The simulations were performed on the basis of online *PPM server*, which can predict the membrane positions of both peripheral and integral proteins [25]. Specifically, spatial arrangement of proteins in membranes is determined by minimizing their transfer energies from water to lipid bilayer. Additional output parameters include the depth of peptide protrusion into the nonpolar membrane region, tilt angle (the angle between the peptide axis and the bilayer normal) and the residues embedded into membrane hydrocarbon core. The calculation is based on the universal solvation model which accounts for hydrophobic, van der Waals, H-bonding and electrostatic solute-solvent interactions [26]. In this model lipid bilayer is represented as a fluid anisotropic medium characterized by dielectric constant (ε), solvatochromic dipolar parameter (π^*), and H-bonding acidity and basicity parameters (α and β). The nonpolar bilayer region of is modeled as a planar slab of adjustable thickness whose interior resembles the decadiene. Interfacial polarity of the membrane is simulated based on EPR, X-ray and spin-labeling experimental measurements of water concentration in the membrane interior [25].

Within the framework of solvation model, the transfer energy of a solute molecule from aqueous phase to the arbitrary position in the membrane accounts for the dependence of the solvation parameters σ_i and η on the atom position along the bilayer normal (z_i), and is given by:

$$\Delta G^{transfer}(d,\varphi,\tau) = \sum_{i=1}^{N} \sigma_i^{wat\to bil}(z_i)\, ASA_i + \sum_{i=1}^{M} \eta_j^{wat\to bil}(z_j)\,\mu_j + \sum_{k=1}^{L} \min\left\{\Delta E_k^{ion}, \Delta E_k^{neutr}\right\}, \quad (2)$$

where $\sigma_i(z_i)$ stands for the solvation parameter, depending on the atom type and describing the surface energy transfer per Å^2 of i-th atom from water to the point z_i on the membrane, ASA_i is a solvent-accessible surface area of i-th atom, $\eta(z_j)$ defines the energy cost of the transferring the dipole moment of 1D from water to point z_j, μ_j – the dipole moment of group j, E_k^{ion} and E_k^{neutr} represent the energies of ionized group k in ionized and neutral states, respectively, N is the number of atoms in the molecule, M is the number of group dipoles, L is the number of ionizable groups, d, φ and τ define the sift along the bilayer normal, rotational and tilt angle, respectively.

The individual dipolar contributions were assumed to linearly decrease to zero when ASA of the atom associated with the dipole moment becomes smaller than the hydration area occupied by a single molecule of water ($ASA_{water} \approx 14$ Å):

$$\Delta G_{dip,j} = \eta_j^{wat\to bil}(z_j)\,\mu_j, \quad \text{if } ASA_j > ASA_{water} \quad (3)$$

$$\Delta G_{dip,j} = \eta_j^{wat\to bil}\left(z_j\right)\mu_j\left(ASA_j / ASA_{water}\right), \quad \text{if} \quad ASA_j \le ASA_{water} \tag{4}$$

Analogous approximation of Born energy for ionized groups yields:

$$\Delta E_k^{ion} = \frac{166 e_{Born}}{r_k}\left[F_{Abe}^{wat} - F_{Abe}\left(z_k\right)\right] f_k + \sum_{i=1}^{L_k}\sigma_{l,ion}^{wat\to bil}\left(z_l\right) ASA_{l,} \quad \text{if} \quad ASA_k > ASA_{water} \tag{5}$$

$$\Delta E_k^{ion} = \frac{166 e_{Born}}{r_k}\left[F_{Abe}^{wat} - F_{Abe}\left(z_k\right)\right]\left(ASA_k / ASA_{water}\right) f_k + \sum_{i=1}^{L_k}\sigma_{l,ion}^{wat\to bil}\left(z_l\right) ASA_{l,} \quad \text{if} \quad ASA_k \le ASA_{water} \tag{6}$$

where coefficient $f_k = 0.5$ if the group is involved in ion pairing, and $f_k = 1$ for the rest of cases.

Analysis of the binding of constructed amyloid fibrils to the lipid membranes allowed us to determine the energetically preferable orientation of the aggregates relative to lipid-water interface, as well as the energetics of protein-lipid binding. Notably, we found it reasonable to analyze not only the most stable structures, but also those covering the entire range of the examined twisting angles.

Table 1

Structural and thermodynamic parameters characterizing membrane location and orientation of **Lz1** and **Lz2** fibrils

Twist angle	ΔG, kcal/mol		Depth*, Å		Tilt angle		Embedded residues	
	Lz1	Lz2	Lz1	Lz2	Lz1	Lz2	Lz1	Lz2
0	-34	-18.8	7	3.9	89	90	I2, L3, W9, I10**	F2, I4, S6
5	-32	-18.4	5.1	4.4	90	87	I2, L3, W9, I10	F2, I4, S6
10	-24	-16.7	4.4	4.7	989	86	I2, L3, W9, I10	F2, I4, S6
15	-16	-16.1	4.2	7.9	87	80	I2, L3, W9, I10	I1 – I4
20	-12.5	-12.4	2.5	5.8	89	82	I2, I10	I1 – I4
25	-12.3	-11.5	2.1	5.2	90	88	I10	I1, F2, S4
30	-11	ND	1.7	ND	90	ND	I10	ND
35	-9.5	-9.8	1.5	5.2	89	87	I10	I1, F2, S4
40	-10.3	-8.2	1.7	5.3	90	90	I10	I1, F2, S4

*depth of penetration into the hydrocarbon core of lipid bilayer

**I10 means the first residue of the second monomer

Table 2

Structural and thermodynamic parameters characterizing membrane location and orientation of of Aβ and A-I fibrils

Twist angle	ΔG, kcal/mol		Depth, Å		Tilt angle		Embedded residues	
	Aβ	A-I	Aβ	A-I	Aβ	A-I	Aβ	A-I
0	-36.6	-26.8	18.4	2	90	88	G17-V23, F28*-I40, G42	L38
5	-34	-23.4	19	2.1	85	88	G17-I24, F28-I41	L38
10	-36.4	-18.8	17.8	3.6	85	87	G17-I24, F28-I40	L38
15	-33.5	-14.9	16.4	4.3	84	83	G17-I24, A30-I41	L38
20	-28.9	-11.9	16.8	4.1	89	79	G17-V22, F29-I40	L38
25	-22.4	-9.9	17.4	4.4	59	81	G17-G21, V33-I40	L38
30	-20	-8.5	19.2	5.3	47	74	G17-V22, V33-I40	L38
35	-23.2	-8.3	23.2	2	14	87	G17-V22, A30-G38	D24, L38
40	-26.2	-8.9	23.8	1.4	7	85	G17-V22, E31-G38	S36, L38

*the residues after 26th belong to the next monomer

Recent experimental data from single molecule atomic force microscopy showed that amyloid periodicity is a tunable parameter whose initial value is sensitive to the changes of experimental variables [23]. In particular, increasing salt concentration was reported to bring about continuous decrease in amyloid pitch, and corresponding twisting angle, according to the dependence:

$$L_2 = L_1\left[\left(\frac{\kappa_1}{\kappa_2}\right)^{1/2} + \frac{\alpha_2}{4\pi}\left(\kappa_1 - \kappa_2\right)L_1^{3/2}\right]^{-2/3}, \tag{7}$$

where L, κ are the fibril pitch of the fibril and inverse Debye length, the subscript denotes salinity regime – 1 or 2 (i.e. ionic strength I_1 or I_2), α_2 is the parameter at ionic strength 2, depending on the intrinsic characteristics of the fibrils (charge density, geometry, elastic rigidity). Elevation of the ionic strength screens the electrostatic interactions within the fibrils and decreases the contribution of the second term in Eq. (1), causing the relaxation of fibril tilt and its untwisting. The weakened electrostatic interactions may alter the H-bonding distribution along the fibrillar aggregates and their mechanical stability, the parameters that also underlie the structural configuration of the amyloid.

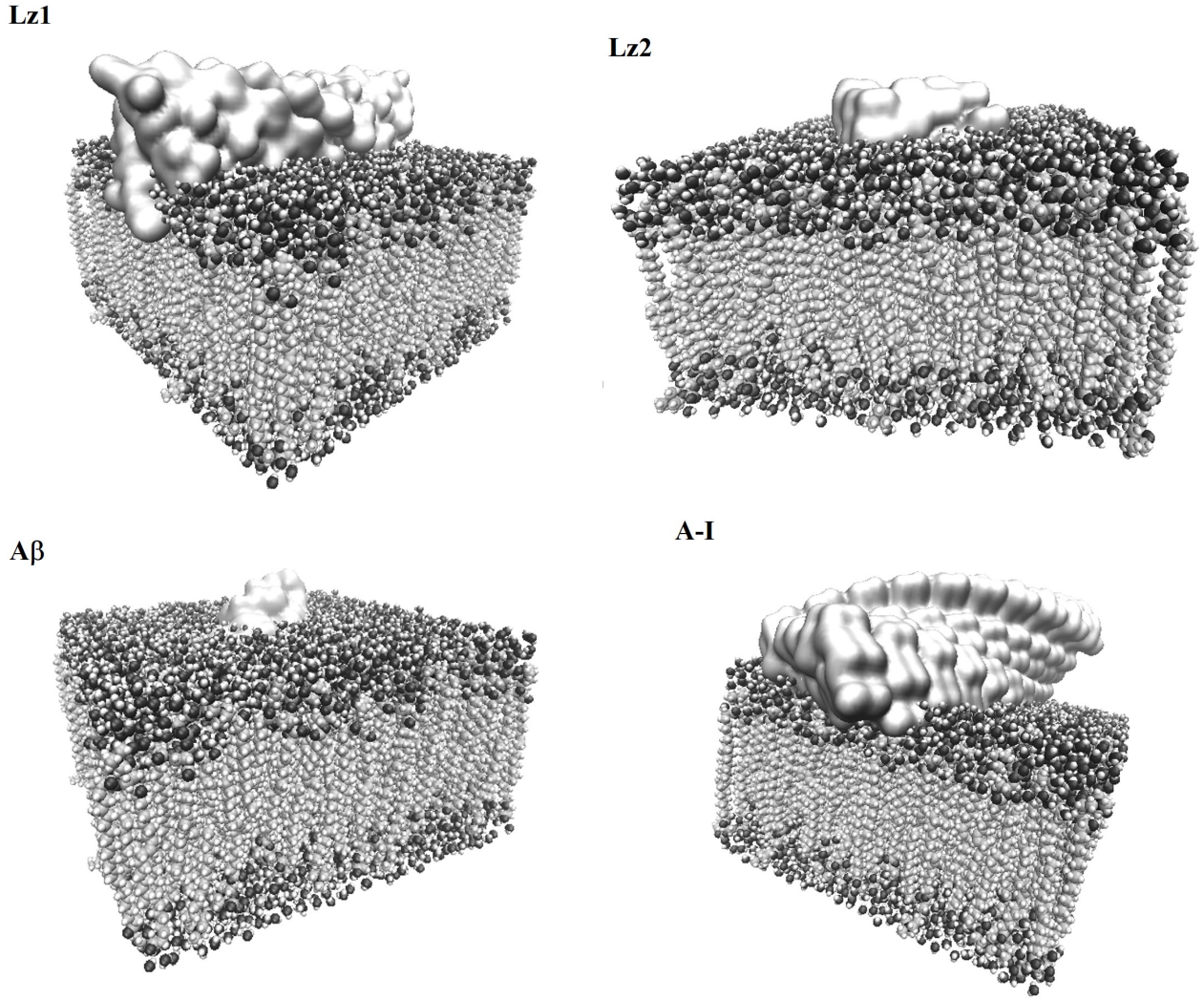

Fig. 3. Representative snapshots of amyloid fibril binding to the lipid bilayers simulated with *PPM* server.

The results of calculations performed with *PPM* are shown in Tables 1, 2, and the representative snapshots are given in Fig. 3. As judged from the tables, the position of amyloid fibrils in the membrane and energetics of peptide-lipid binding is strongly determined by amino acid sequence and the twist of the polypeptide chain. The recovered values of the tilt angle indicate that preferable orientation of amyloid fibrils from **Lz1**, **Lz2** and **A-I** peptides is parallel or slightly tilted with respect to the bilayer surface. In contrast, **Aβ** fibrils were found to reside parallel to membrane surface only up to twisting angle of *ca.* 20°, while further increase in θ was followed by the rise in tilt angle up to 7° (Table 2), the value corresponding to almost perpendicular orientation to the bilayer surface.

Furthermore, the general tendency observed for all peptides is the decrease in transfer energy upon increasing twisting angle of the fibrils. This means that it is becoming energetically unfavorable for the peptide to insert into the lipid bilayer with increasing its periodicity and amyloid fibrils tend to locate at lipid/water interface or in the membrane polar region. This effect can be explained by at least two factors. The first one is that different amino acid residues participate in peptide-lipid binding depending on the fibril twist. According to White-Wimley hydrophobicity scale, the free energy of transfer of individual amino acid residues from water to the lipid phase varies substantially from residue to residue and is controlled by residue charge, chemical structure and its polarity [27]. If one take, for the sake of illustration, the peptide **Lz1** and calculate roughly the sum of transfer energy contributions from each residue (see Fig. 8C in [27] for the values of transfer energies for each amino acid) taking part in membrane penetration (ΔG^{sum}), it appears that at $\theta = 5^{\circ}$, $\Delta G^{sum} = \Delta G^{I2} + \Delta G^{L3} + \Delta G^{W9} + \Delta G^{I10} = -0.31 - 0.56 - 1.85 - 0.31 = -3.03$ kcal/mol, while at $\theta = 40^{\circ}$ $\Delta G^{sum} = \Delta G^{I10} = -0.31$ kcal/mol. Analogously, for **A-I** fibrils at $\theta = 5^{\circ}$ $\Delta G^{sum} = \Delta G^{L38} = -0.56$ kcal/mol, while at $\theta = 40^{\circ}$ $\Delta G^{sum} = \Delta G^{L38} + \Delta G^{D24} = -0.56 + 1.23 = 1.59$ kcal/mol. These calculations show that variation even in one amino acid residue, being in contact with nonpolar bilayer region may significantly change the free energy of transfer. Furthermore, one should bear in mind that the difference in ΔG^{sum} (and, as a consequence, the overall $\Delta G^{transfer}$) in our systems may be further increased if one takes into account the inter-residue interactions within the fibrils, their structural peculiarities, as well as the other constituents of total transfer energy, the factors that were neglected upon these rough calculations and that may substantially change the transfer energy of individual residues. However, evidently, the difference in the nature of amino acid residues, protruding the membrane hydrophobic region, is not the only reason for the observed increase in absolute values of $\Delta G^{transfer}$. Specifically, for all peptides we observed the rise in free energy at increasing twisting angle that was not accompanied by the change in amino acid residues embedded into nonpolar core of lipid bilayer. For example, in the case of **Lz1** elevation of the twisting angle from 5 to 15 degrees resulted in two-fold increase in $\Delta G^{transfer}$ despite the observation, that amino acid residues penetrating the acyl chain region were the same in both cases (Table 1). This finding can be rationalized in terms of the alterations in physicochemical and structural properties of the amino acid residues (such as *ASA*, the ability to form H-bonds, polarity characteristics, arrangement in β-stacks, etc.) upon increasing the twisting angle.

Notably, modeling of increasing twist of peptide aggregates may resemble the maturation of amyloid from oligomeric nucleus. At the beginning of fibril growth phase, the protofilaments have a flat structure, and their intertwining is rare and random across the contour length. However, the magnitude of twisting angle and the number of twisting points increases with incubation time [12]. Furthermore, according to the prevailing concepts, amyloid intermediates (oligomeric aggregates with small twist) are thought to have much more pronounced impact on membrane structure compared to mature fibers with high twist. In view of this, the findings outlined here, may provide the possible explanation for this phenomenon, i.e. it is thermodynamically unfavorable for grown fiber to penetrate the membrane, since its twisted structure would require much more energy for membrane to adjust its contact region to the intertwined structure of the fibrils.

CONCLUSIONS

1) Based on the different computational approaches, in the present work we constructed the core region of amyloid fibrils from hen egg white lysozyme, Aβ-peptide and apolipoprotein A-I, and analyzed their association with lipid membranes.
2) Simulation of the amyloids using the *CreateFibril* software showed that all fibrillar aggregates are characterized by the repeated twisted β-stacked structure, a characteristic signature of amyloid assembly. Subsequent evaluation of fibril free energy on the basis of *AQUASOL* server allowed identifying the twisting angle ensuring the most stable structure for every of the examined peptides.
3) Modeling fibril-lipid interactions with *PPM* tool showed that elevating amyloid twist results in increasing transfer energy of the peptide from water to lipid environment. The molecular determinants of this observation were supposed to involve chemical structure, ASA and the number of amino acid residues penetrating the membrane hydrocarbon core.

The obtained results may prove to be useful in elucidation the molecular-level details of amyloid cytotoxicity mechanisms.

REFERENCES

1. Harrison R.S., Sharpe P.C., Singh Y., Fairlie D.P. Amyloid peptides and proteins in review // Rev. Physiol. Biochem. Pharmacol. – 2007. – Vol. 159. – P. 1-77.
2. Chiti F. Dobson C. Protein misfolding, functional amyloid, and human disease // Ann. Rev. Biochem. – 2006. – Vol. 75. – P. 333-366.
3. Pham C.L.L., Kwan A.H., Sunde M. Functional amyloid: widespread in nature, diverse in purpose // Essays Biochem. – 2014. – Vol. 56. – P. 207-219.

4. Wei W., Wang X., Kusiak J.W. Signaling events in amyloid β-peptide-induced neuronal death and insulin-like growth factor I protection // J. Biol. Chem. – 2002. – Vol. 277. – P. 17649-17656.
5. Nelson R., Sawaya M., Balbirnie M., Madsen A., Riekel C., Grothe R., Eisenberg D. Structure of the cross-beta spine of amyloid-like fibrils // Nature. – 2005. – Vol. 435. – P. 773-778.
6. Makin O., Atkins E., Sikorski P., Johansson J., Serpell L. Molecular basis for amyloid fibril formation and stability // Proc. Natl. Acad. Sci. USA. – 2005. – Vol. 105. – P. 315-320.
7. Lara C., Adamcik J., Jordens S., Mezzenga R. General self-assembly mechanism converting hydrolyzed globular proteins into giant multistranded amyloid ribbons // Biomacromolecules. – 2011. – Vol. 12. – P. 1868-1875.
8. Usov I., Adamcik J., Mezzenga R. Polymorphism in bovine serum albumin fibrils: morphology and statistical analysis // Faraday Discuss. – 2013. – Vol. 166. – P. 151-162.
9. Aggeli A. Hierarchical self-assembly of chiral rod-like molecules as a model for peptide β-sheet tapes, ribbons, fibrils, and fibers // Proc. Natl. Acad. Sci. USA. – 2001. – Vol. 98. – P. 11857-11862.
10. Nyrkova I. Self-assembly and structure transformations in living polymers forming fibrils // Eur. Phys. J. B. – 2000. – Vol. 17. – P. 499-513.
11. Periole X., Rampioni A., Vendruscolo M., Mark A. Factors that affect the degree of twist in β-sheet structures: a molecular dynamics simulation study of cross-β filament of the GNNQQNY peptide // J. Phys. Chem. B. – 2009. – Vol. 113. – P. 1728-1737.
12. Adamcik J., Mezzenga R. Protein fibrils from a polymer physics perspective // Macromolecules. – 2012. – Vol. 45. – P. 1137-1150.
13. Petkova A. Self-propagating, molecular-level polymorphism in Alzheimer's beta-amyloid fibrils // Science. – 2005. – Vol. 307. – P. 262-265.
14. Zerovnik E. Amyloid-fibril formation. Proposed mechanisms and relevance to conformational disease // Eur. J. Biochem. – 2002. – Vol. 269. – P. 3362-3371.
15. Trusova V., Gorbenko G., Girych M., Adachi E., Mizuguchi C., Sood R., Kinnunen P., Saito H. Membrane effects of N-terminal fragment of apolipoprotein A-I: a fluorescent probe study // J. Fluoresc. – 2015. – Vol. 25. – P. 253-261.
16. Kastorna A., Trusova V., Gorbenko G., Kinnunen P. Membrane effects of lysozyme amyloid fibrils // Chem. Phys. Lipids. – 2012. – Vol. 165. – P. 331-337.
17. Smaoui M. Computational assembly of polymorphic amyloid fibrils reveals stable aggregates // Biophys. J. – 2013. – Vol. 104. – P. 683-693.
18. Schneidman-Duhovny D., Inbar Y., Nussimov R., Wolfson H. PatchDock and SymmDock: servers for rigid and symmetric docking // Nucl. Acids Res. – 2005. – Vol. 33. – P. W363-W367.
19. Andrusier N., Nussimov R., Wolfson H. FireDock: fast interaction refinement in molecular docking // Proteins. – 2007. – Vol. 69. – P. 139-159.
20. Girych M., Gorbenko G., Trusova V., Adachi E., Mizuguchi C., Nagao K., Kawashima H., Akaji K., Lund-Katz S., Phillips M., Saito H. Interaction of Thioflavin T with amyloid fibrils of apolipoprotein A-I N-terminal fragment: resonance energy transfer study // J. Struct. Biol. – 2014. – Vol. 185. – P. 116-124.
21. Koehl P., Delarue M. AQUASOL: an efficient solver for the dipolar Poisson-Boltzmann-Langevin equation // J. Chem. Phys. – 2010. – Vol. 132. – P. 064101-064117.
22. Dzwolak W., Pecul M. Chiral bias of amyloid fibrils revealed by the twisted conformation of Thioflavin T: an induced circular dichroism/DFT study // FEBS Lett. – 2005. – Vol. 579. – P. 6601-6603.
23. Adamcik J., Mezzenga R. Adjustable twisting periodic pitch of amyloid fibrils // Soft Matter. – 2011. – Vol. 7. – P. 5437-5443.
24. Sunde M. Common core structure of amyloid fibrils by synchrotron X-ray diffraction // J. Mol. Biol. – 1997. – Vol. 273. – P. 729-739.
25. Lomize M., Pogozheva I., Joo H., Mosberg H., Lomize A. OPM database and PPM web server: resources for positioning of proteins in membranes // Nucl. Acids Res. – 2012. – Vol. 40. – P. D370-D376.
26. Lomize A., Pogozheva I., Mosberg H. Anisotropic solvent model of the lipid bilayer. 2. Energetics of insertion of small molecules, peptides, and proteins in membranes // J. Chem. Inf. Model. – 2011. – Vol. 51. – P. 930-946.
27. White S., Whimley W. Membrane protein folding and stability: physical principles // Annu. Rev. Biophys. Biomol. Struct. – 1999. – Vol. 28. – P. 319-365.